# Investigation of Neuraminidase-Substrate Recognition Using Molecular Dynamics and Free Energy Calculations

Kevin M. Masukawa, Peter A. Kollman,[†] and Irwin D. Kuntz*

*Department of Pharmaceutical Chemistry, Chemistry and Chemical Biology Program, University of California, San Francisco, 600 16th Street, Box 2240, San Francisco, California 94143-2240*

Development of the new generation of therapeutics against the influenza viral coat protein neuraminidase is a response to the continuing threat of influenza epidemics. A variety of structurally similar compounds have been reported that vary greatly in their ability to inhibit neuraminidase, a critical enzyme that cleaves sialic acid and promotes virion release. To determine how neuraminidase exhibits this wide range of affinities with structurally similar compounds, molecular dynamic simulations, coupled with free energy calculations, were used to determine the binding components of a series of neuraminidase inhibitors. Using four cocrystal structures of neuraminidase−inhibitor complexes, we examined the structural and energetic components of ligand potency and selectivity. An in-depth energetic analysis, including internal energy, entropy, and nonbonded interactions, reveals that potency of ligand binding is governed by nonpolar contacts. Electrostatic components generally oppose binding, although two of the best inhibitors use electrostatic interactions to orient the ligand. This investigation suggests that the enhanced selectivity and potency of the better ligands may arise from an improved positioning of their ligand atoms in the active site due to polar and hydrophobic functionalities. Simulations that included crystal water molecules in the active site indicate that the more potent ligands make less use of water-mediated interactions.

## Introduction

The viral disease influenza afflicts millions of individuals each year. Current therapeutics, including both vaccines and drugs, have curtailed the deaths once associated with the virus, but despite these advances in treatment, the threat of resistance from antigenic shifts or drifts provokes the need for new treatment modalities. The influenza virus uses a pair of carbohydrate binding proteins, hemagglutinin and neuraminidase, to initiate viral fusion and subsequent budding of new virions from the infected cell.[1,2] Both of these glycoproteins are present on the surface of the influenza virus and are essential for virion propagation. Hemagglutinin recognizes target cells via sialic acid binding sites and then promotes viral fusion.[3] Neuraminidase cleaves terminal sialic acid moieties of virus progeny to promote the release and subsequent spreading of new virus particles.[4] Both glycoproteins have been suggested as therapeutic targets to prevent the spread of the influenza virus in the host.[5−7] Unlike hemagglutinin, neuraminidase has enzymatic constraints that reduce the frequency of resistant strains. To date, more success has been achieved designing compounds against neuraminidase than hemagglutinin.[8−14] Due to its role in the life cycle of the influenza virus, and its potential to prevent the spread of infection, neuraminidase is an appealing target.

Neuraminidase exhibits a high degree of selectivity among structurally similar compounds. Despite binding its natural ligand, sialic acid, with only millimolar affinity,[15,16] designed inhibitors of neuraminidase bind with a much higher affinity, sometimes reaching the low nanomolar range.[8,14,17,18] Figure 1 shows four inhibitors of neuraminidase exhibiting a broad range of binding affinities; the difference between the best binding ligand, Tamiflu, and the worst binding ligand, sialic acid, is over 12 kcal/mol. Currently, crystal structures of neuraminidase with these four inhibitors bound are available. Upon looking at these structures, their different recognition elements are not apparent; all four inhibitors bind in the same pocket and interact with the same set of residues. To exploit further the binding properties of neuraminidase for inhibitor design, a detailed analysis of how neuraminidase recognizes these structurally similar ligands with such large variation in binding affinity needs to be performed. In the past, the lack of structural data has forced researchers to use reduced representations of the neuraminidase binding site in attempts to elucidate the foundation of this binding affinity differential. These theoretical efforts, using pharmacophore[9] or protein structure-based models,[19,20] used simplified scoring functions that neglected the contributions from internal conformational strain, entropy, or water interactions to the binding free energy. Considering the dynamic and amphipathic nature of carbohydrates, these missed contributions may be significant. Given the availability of four high-resolution X-ray cocrystal structures of neuraminidase with bound inhibitor, we decided to use advanced methods to quantify these interactions.

Here we report a detailed analysis of neuraminidase−inhibitor interactions using the computational technique developed in its current form in the Case and Kollman laboratories known as Molecular Mechanic Poisson−

* To whom correspondence should be addressed. Tel: (415) 476−1937. Fax: (415) 502−1411. Email: kuntz@cgl.ucsf.edu.
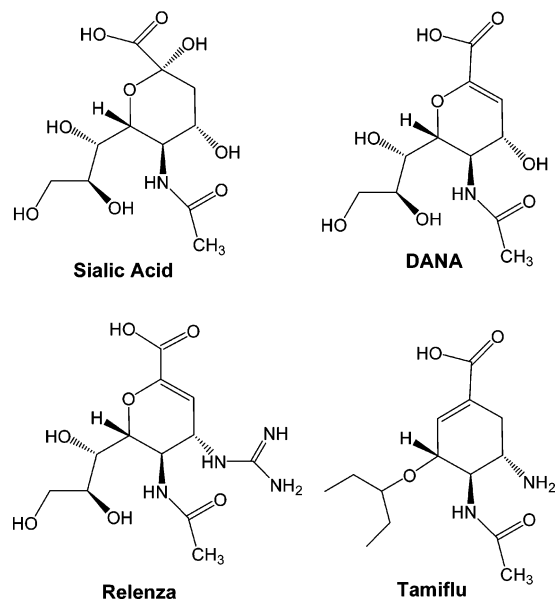† Deceased.

**Figure 1.** Neuraminidase ligands studied in this investigation. Experimental values given as $IC_{50}$'s, except for sialic acid.[8,16] Sialic Acid = 6.1 mM, DANA = 10 $\mu$M, Relenza = 0.3–2.3 nM, Tamiflu = 0.01–2.2 nM.

Boltzmann Surface Area (MM/PBSA). This method, like others,[21,22] utilizes a combination of molecular dynamic simulations and free energy calculations to predict the free energy of a system based on its conformation. MM/PBSA has had great success explaining receptor–ligand interactions at the atomic level.[23–26] Molecular dynamics permits probing structural questions beyond what is possible from direct observation of the static crystal structure model alone. In this study, molecular dynamics and MM/PBSA calculations were performed on a series of sialic acid analogues bound to neuraminidase (Figure 1). The purpose of this investigation is to determine which thermodynamic quantities drive complexation and how these contributions differ among different ligands. The information gained from this analysis could lead to the discovery of new inhibitors with improved binding properties. Using this computational technique we also investigate the role structural waters play in mediating these interactions.

## Computational Methodology

**Abbreviations.** DANA, 2-deoxy-2,3-didehydro-*N*-acetylneuraminic acid (Neu5Ac2en); MM/PBSA, Molecular Mechanic Poisson- Boltzmann Surface Area; Relenza, 2,4-dideoxy-2,3-didehydro-4-guanidino sialic acid (zanamivir); Tamiflu, ethyl 4-acetamido-5-amino-3-(1-ethylpropoxy)-1-cyclohexene-1-carboxylate (oseltamivir) (Note: Tamiflu is the ethyl ester of ethyl 4-acetamido-5-amino-3-(1-ethylpropoxy)-1-cyclohexene-1-carboxylate, our study focuses on the active form of Tamiflu, the carboxylate, interacting with neuraminidase.)

**System Setup.** Atomic coordinates for all cocrystal complexes were obtained from the Protein Data Bank (PDB). Raw crystal structures were modified for dynamics using the LEAP module in Assisted Model Building with Energy Refinement (AMBER 6.0).[27] Four different crystal structures of neuraminidase bound to different inhibitors were used as starting structures in this study. The inhibitors were

sialic acid (1MWE[28]), DANA (1F8B[29]), Relenza (1NNC[30]), and Tamiflu (2QWK[31]). All structures are cocrystal complexes of the avian influenza virus A, subtype N9 at pH 7.0. In the LEAP module of AMBER, protons were added to the system. In accord with crystallographic conditions of the complexes, all ionizable side chains were configured in their characteristic ionized states at pH 7.0. All histidines were singly protonated at the $\delta$ nitrogen. The binding site of neuraminidase has been seen to accommodate crystal waters when binding different ligands. Active site structural waters present in the crystal structure were not removed from the coordinate file if they lie between the ligand and protein. This treatment was justified by observing that solvent-exposed waters diffuse into bulk solvent on our simulation time scale while buried waters do not. No restraints were placed on the crystallographic water molecules during the simulations. Sequestered water molecules were free to move, but did not diffuse out of the pocket over the length of the simulation. Directionality of the hydrogen bonds was random during the initial setup but was allowed to optimize during the equilibration. Structures were then solvated with a water cap (TIP3P)[32] out to 30 Å from the inhibitor while maintaining crystal water positions. The dielectric constant in all simulations was set to 1 because explicit water molecules were added. To test the structural effects of these crystal water molecules, simulations were also performed with no water molecules within the protein–ligand interface. In those cases, all crystal waters were removed before the addition of cap water molecules, which were themselves excluded from being between the protein and ligand.

Atomic partial charges for the four ligands were derived for this study using the RESP method.[33] To obtain minimized geometries for electrostatic potential calculations, ligand geometries were first optimized with Gaussian98 using the Hartree–Fock/6-31G* level of theory.[34] Single-point calculations with Gaussian98 were then performed to obtain the electrostatic potential around each compound using the same basis set and level of theory as in the optimization step. Fitting charges to the electrostatic potential was then performed with RESP. Sialic acid and DANA were both given a formal charge of −1 while Relenza and Tamiflu had 0. Equivalent atoms were given equal partial charges. Amino acid charges came from the RESP derived AMBER94 database.

**Simulations.** Molecular dynamics (MD) produces a time trajectory of the system by solving Newton's equations of motion for each atom. All MD simulations were performed using the SANDER module in the AMBER 6.0 suite of programs. An all-atom representation of the system was used employing the Cornell et al.[35] force field to assign parameters for the standard amino acids. A "belly" region of 17 Å was defined around the ligand. During the simulations these "belly" atoms, which are less than 17 Å from the ligand, were allowed to move, while all atoms beyond 17 Å were held rigid. Structures were first allowed to relax under steepest decent minimization for 10 cycles, followed by a conjugant gradient minimization for 4990 cycles. Upon minimization, the water cap was equilibrated for 10 picoseconds (ps) to allow cavities in the protein to

become solvated. The entire Belly region was then equilibrated for 100 ps with the system gradually warmed to 300 K over the initial 50 ps. Production MD was performed for a nanosecond (ns) with a 2 fs time step and the SHAKE algorithm[36] holding all bond lengths fixed. During the simulation, nonbonded cutoffs were set to 12 Å, the temperature was maintained at 300 K.

Due to the flexible nature of some of the ligands, it is incorrect to assume that the ligand conformations are the same in the bound state versus free in solution. The solution conformations of the ligands were determined with separate simulations. Initial ligand conformations were taken directly from the cocrystal structures with neuraminidase. The ligands were then minimized and equilibrated using the same number of cycles used to optimize the complexes. Upon equilibration, ligands were simulated for 1 ns at 300 K in a box with 8.0 Å of water surrounding each ligand. The conformations generated from this set of simulations were used to calculate energies associated with ligands free in solution.

**Energetic Analysis.** Utilizing the trajectory generated by molecular dynamics, free energy calculations were performed using a Molecular Mechanic/ Poisson– Boltzmann Surface Area scoring function to determine binding affinities as well as component energy contributions. Free energies of binding were determined by calculating internal energy changes upon binding using the AMBER program with the Cornell et al. force field coupled with a continuum solvent model to evaluate free energies of solvation. An estimate of the absolute free energy of binding, $\Delta G_{\text{Bind}}$, is obtained by taking the difference of the complex energy minus the separate reactants' energies.

$$\Delta G_{\text{bind}} = \overline{G}_{\text{complex}} - (\overline{G}_{\text{receptor}} + \overline{G}_{\text{ligand}}) \qquad (1)$$

The average free energy of the complex, receptor, or ligand used in the above equation is composed of the molecular mechanic, solvation, and entropic energies of the system over the trajectory and is represented by the following equation.

$$\overline{G} = \overline{E}_{\text{MM}} + \overline{G}_{\text{solv}} - T\overline{S} \qquad (2)$$

$$\overline{E}_{\text{MM}} = \overline{E}_{\text{bond}} + \overline{E}_{\text{angle}} + \overline{E}_{\text{dihedral}} + \overline{E}_{\text{VDW}} + \overline{E}_{\text{elec}} \qquad (3)$$

$E_{\text{MM}}$ is the molecular mechanical energy obtained from bonded and nonbonded interactions within the system. $G_{\text{solv}}$ represents the electrostatic and nonpolar free energy of solvation and TS is the solute entropic contribution to the system at temperature $T$ (Kelvin). All energies represented in the above equations are averaged over the course of the molecular dynamics trajectories.

The continuum model for the free energy of solvation uses a finite-difference Poisson–Boltzmann approach to calculate the electrostatic energy, coupled with a surface area dependent term for the nonpolar contribution to solvation. Ultimately, the molecular dynamics trajectory is split into "snapshots", stripped of all noncrystal water molecules, and evaluated individually using this scoring scheme. In the energetic analysis, crystallographic

waters were considered as an extension of the protein. Using snapshots from an extended simulation to generate binding energies will allow us not only to sample the flexibility of the binding site, but also to obtain a more reliable free energy estimate of binding than compared to a single snapshot calculation.

Entropic contributions to binding were determined using a normal mode approximation.[37–39] The change in solute entropy upon association was estimated by calculating normal-mode frequencies using the NMODE module within AMBER6.0. For each complex five snapshots from the MD trajectories were taken at 100 ps intervals and a region defined by a 17 Å sphere from the inhibitor was used for the entropy analysis. Each snapshot was minimized using a distant-dependent dielectric, 4r, before normal mode analysis. Solvent entropies of the system are implicitly included in the nonpolar and polar solvation free energy terms.

The binding free energy was calculated by taking the difference in MM/PBSA energy for the ligand–protein complex and uncomplexed reactants. From the 1 ns simulations, snapshots were collected every 10 ps. Ligated and apo protein conformations were obtained from the simulations of the complex, while the unbound ligand conformations were obtained from a separate trajectory, as described above. MM/PBSA scores for each of these snapshots were averaged to obtain a free energy of association. The molecular mechanic (MM) energy was obtained using the Cornell et al. force field as implemented in AMBER with no cutoffs. The Poisson– Boltzmann solvation energy was calculated with the DELPHI program[40] using a grid spacing of 0.5 Å, 80% fill of the grid box, and an exterior dielectric of 80. While the exact value of the interior dielectric constant remains to be unequivocally established, a recent MM/ PBSA study in protein structure prediction showed an improved correlation with experiment when the protein interior was modeled with a dielectric of 4 versus 1.[41] This result coupled with the solvent accessibility of the neuraminidase active site and the calculations of Jedrezjas et al.[15] support the use of an interior dielectric constant of 4 for our study. Nonpolar contributions to solvation were estimated as a function of the solvent-accessible surface area (SASA). The solvent-accessible surface area is calculated using the MSMS program[42] and the nonpolar contribution to the free energy of binding is given by

$$\Delta G_{\text{solv}}^{\text{nonpolar}} = \gamma(\text{SASA}) + b \qquad (4)$$

where SASA is the solvent-accessible surface area and $\gamma$ and $b$ are constants. The values for $\gamma$ and $b$ were derived experimentally from the transfer of small hydrocarbons by Sitkoff et al.[43] and are 0.00542 kcal/ mol·A² and 0.92 kcal/mol, respectively.

**Computational Alanine-Scanning.** From the wild-type trajectory, snapshots were generated every 10 ps for alanine-scanning. Mutations to alanine were performed only on selected residues in the active site. Alanine mutations were generated by truncation of residues after the C$\beta$ and adding a hydrogen in the same direction as the C$\gamma$. Partial charges for the mutated residue were then changed to those of alanine. None of the residues mutated in this study were glycines.

**Table 1.** Average Energy Contributions (kcal/mol) to the Free Energy of Binding for Neuraminidase and the Set of Four Ligands[a]

| contribution | Tamiflu | Relenza | DANA | sialic acid |
|---|---|---|---|---|
| $\Delta E_{internal}$[b] | −6.07 (0.51) | 1.90 (0.68) | −5.36 (0.53) | 5.16 (0.48) |
| $\Delta E_{VDW}$[c] | −29.16 (0.48) | −29.99 (0.51) | −23.13 (0.56) | −23.32 (0.47) |
| $\Delta E_{elec,internal}$[d] | −44.49 (0.52) | −58.49 (0.39) | −35.15 (0.53) | −44.91 (0.28) |
| $\Delta G_{elec,solv}$[e] | 46.81 (0.42) | 58.22 (0.27) | 38.46 (0.39) | 45.4 (0.21) |
| $\Delta G_{nonpolar,solv}$[f] | −4.46 (0.01) | −4.65 (0.01) | −4.12 (0.01) | −4.13 (0.01) |
| $\Delta E_{elec,int+solv}$[g] | 2.31 (0.17) | −0.26 (0.22) | 3.31 (0.24) | 0.49 (0.21) |
| $-T\Delta S$[h] | 21.6 (1.35) | 19.6 (1.56) | 22.4 (1.64) | 20.11 (1.47) |
| $\Delta G_{bind}$[i] | −15.78 (1.49) | −13.4 (1.63) | −6.90 (1.70) | −1.69 (1.58) |
| $\Delta G_{bind\ experiment}$[j] | −15.2 to −12.0 | −13.2 to −11.9 | −6.91 | −3.06 |

[a] Obtained from trajectories that included crystal waters. Errors are given as standard errors of the mean. [b] Internal contributions from bond, angle, and dihedral terms. [c] Nonbonded van der Waals. [d] Nonbonded electrostatics. [e] Electrostatic component to solvation. [f] Nonpolar component to solvation. [g] Total electrostatic change upon binding. [h] Entropic contributions to binding. [i] Total change of free energy in binding. [j] References 8, 16. Experimental data given as IC$_{50}$s for all ligands except sialic acid. For direct comparison to calculated affinities, conversion to $\Delta G$ estimated by $\Delta G = -RT \ln$ IC$_{50}$.

## Results and Discussion

**Energetic Analysis.** Using a combined MD/MMPB-SA approach, our calculations show an excellent correlation with experimental results (Table 1). Table 1 shows the binding free energy components averaged over the MD trajectory for each cocrystal complex. Along with discriminating the worst ligand, our calculations also agree with the experimental finding that Tamiflu is the best binding ligand. All ligands are correctly rank-ordered and the magnitudes of the $\Delta G$s are in good agreement with experiment.

If we examine the contributions to binding across the ligand series, there is an increase in the van der Waals contribution as the interaction becomes more favorable. This appears to explain the affinity progression because while all other nonbonded binding components remain relatively constant across the series, the tightly bound ligands have added nonpolar packing in the active site. The better binding Tamiflu and Relenza gain over 6 kcal/mol more van der Waals energy over their less potent counterparts, DANA and sialic acid. Interestingly, the presence of the large ether moiety in Tamiflu does not increase its overall van der Waals interaction energy compared to that of Relenza. As will be discussed below, our simulations with crystal waters suggest that the ether moiety may facilitate better positioning of Tamiflu in the active site. The importance of nonpolar interactions in targeting neuraminidase was also identified in previous investigations.[10,12,44] Further analysis of the binding components reveals that while the van der Waals and nonpolar solvation energies drive binding for all four ligands, sterics alone do not completely explain the affinity differential.

We also find that the overall electrostatic component to binding either provides no thermodynamic benefit or even opposes association despite the large number of polar groups in the active site. Of the four compounds studied, the only ligand that has a favorable electrostatic component to binding is Relenza ($\Delta E_{elec}$= −0.26 kcal/mol). It appears that Relenza gains this electrostatic energy by having a large positive guanidinium group that interacts favorably with E227 at the bottom of the active site. Favorable internal electrostatic energy is gained as one proceeds from a hydroxyl (DANA) off the C4 position to an ammonium (Tamiflu), and guanidinium group (Relenza). However, the inclusion of desolvation effects leads to a net *loss* of binding except for Relenza. The importance of including desolvation

penalties when calculating binding affinities to this receptor is reinforced by work done by Smith et al. who reported that the addition of charge to various DANA analogues was deleterious to binding.[29] For example, it costs more for DANA in electrostatic energy to bind to neuraminidase than sialic acid, 3.31 kcal/mol versus 0.49 kcal/mol (Table 1). This is most likely due to DANA's lack of flexibility that precludes optimal charge complementarity in the active site to offset desolvation penalties, as evident by DANA's Coulombic interaction energy being less than that for sialic acid, −35.15 versus −44.91 (Table 1). Where others have noted the importance of a positively charged group off the C4 position,[20,45] our work suggests that the benefit from adding these groups might not be solely from electrostatic interactions. The fact that Tamiflu is the most potent binder, despite Relenza having more favorable nonbonded interactions, suggests that internal strain energy is also an important factor in increased affinity and selectivity, as shown below.

**Energetic Analysis of Free Ligands.** Our studies of the free ligands in separate trajectories provide an estimate for the local adaptation energy upon complex formation. Along with internal changes in van der Waals, Coulombic, and solvation energy, free ligand trajectories enable an estimation of the ligand strain upon binding. Ligand strain is defined as the difference in bond, angle, and dihedral terms between the conformation in the bound state and the conformation free in solution. Sialic acid contains a pyranose ring, which due to its flexible nature can populate many conformations in solution that vary greatly in energy. In the neuraminidase−sialic acid cocrystal structure, sialic acid is bound in a boat/twist-boat conformation, which is higher in energy than its chair form. Upon binding, the internal energy associated with the conformational change in the pyranose ring of sialic acid is calculated to cost roughly 5.0 kcal/mol in binding free energy. This penalty is much larger than compared to the other three inhibitors. The unfavorable strain energy upon binding is a major component of why sialic acid has a lower affinity for neuraminidase than DANA; the difference experimentally is roughly 2.5 kcal/mol for the pyranose ring only.[46] With the inclusion of the double bond in the pyranose ring, DANA does not experience a large conformational strain increase upon binding compared to its conformation in the free unbound form. Disregarding energetic terms associated with the ligands free in solution, both

**Table 2.** Internal Strain Energy Change (kcal/mol) of Ligands upon Binding Neuraminidase

|  | acetyl group | central ring |
|---|---|---|
| sialic acid | 0.12 | 1.69 |
| DANA | −0.66 | −2.57 |
| Relenza | 4.59 | −0.84 |
| Tamiflu | −0.81 | −1.85 |

DANA and sialic acid have similar calculated interaction energies, −26.95 and −27.17 kcal/mol, respectively (data not shown).

Just as DANA and sialic acid have strain energies to discern the two interactions, the same type of thermodynamic component also differentiates Tamiflu and Relenza. Tamiflu has a reduction in strain energy of −6.07 kcal/mol upon binding where Relenza pays 1.90 kcal/mol upon association. A further investigation reveals that much of the costs in internal energy is due to Relenza straining the acetyl group conformation upon binding. Tamiflu and the other two weaker binders do not experience a large strain on the acetyl group like that of Relenza (Table 2). As will be discussed further, the strain on Relenza can be attributed to its dependence on waters for positioning in the active site.

Negative changes in strain energy upon complex formation are a result of the ligand binding in a conformation that is more favorable in the protein than outside. One explanation is that the enzyme site is preorganized to favor the bound geometry. Alternatively, Tamiflu's ammonium group may contribute to its strained geometry in solution. The high charge density maintains a close interatomic distance to the carbonyl of the acetyl group in solution. Upon binding, this distance is increased by 0.2 Å on the average, lowering the strain on the ligand. Relenza, with the larger positively charged guanidinium group, does not induce a strained conformation in solution. Once bound, this guanidinium group shifts to charge complement E227, reducing the distance between the guanidinium and acetyl group adding strain on the ligand. DANA which also experiences a negative strain energy upon binding, undergoes a similar conformational strain reduction to Tamiflu. Interestingly, sialic acid encounters the same type of shift in distance, but perhaps its flexible ring prevents a large strain from being incurred in solution. As mentioned above, sialic acid's overall unfavorable binding strain is mainly contributed from the large ring flip induced upon binding. Due to the charged nature and large number of hydrogen bond donors and acceptors of these ligands, strained conformations in solution are not unexpected.

Given the large dimensionality of conformational space available to each ligand, a true estimate for the adaptation energy requires a higher sampling technique. The energetic contributions from the free ligand conformations generated through MD simulations are most likely overestimates of the underlying adaptation energy. Although local, inclusion of this ligand conformational energy using MD simulations allows an estimate for the adaptation energy each ligand experiences upon binding, regardless of the exact molecular mechanism. Clearly, these ligands in solution must be treated as an average over an ensemble of the conformations.

**Role of Crystal Water Molecules.** Carbohydrate binding proteins commonly use water molecules to mediate their interactions with ligands; the role these waters play has yet to be fully elucidated.[47−50] In each of the four cocrystal structures, at least three crystallographic water molecules are seen trapped between neuraminidase and its inhibitor. To investigate their role in these recognition events, we performed a series of simulations with and without these crystal waters present in both the MD simulations and postprocessing. By performing a set of simulations without water molecules between the protein and ligand, we can isolate structural perturbations in the active site that are directly related to the absence of these waters. This investigation revealed that with three of the four ligands, crystal waters are necessary to stabilize the ligand orientation in the active site (Figure 2). The RMSD plots of the ligand positions during MD simulations with and without crystal waters suggest that the weaker binders are more dependent on waters to mediate their interactions than the best binder, Tamiflu (Figure 2). In both sialic acid and DANA, the central ring shifts position in the absence of crystal waters, which alters the placement of some functional groups relative to their positions when crystal waters are included.

Relenza also experiences a minor displacement with crystal waters removed by undergoing a different type of movement compared to sialic acid or DANA. Upon inspection, it is apparent that much of the displacement of Relenza arises from the glycerol group shifting to compensate for water not being present (Figure 3). The guanidinium group, on the other hand, is situated deep in the active site and occupies the same space irrespective of water molecules being present or absent. Thus, Relenza appears to partially overcome crystal water dependence by having the positively charged guanidinium group anchor the entire ligand in the active site. Comparing the bound ligand conformations between simulations performed with and without crystal waters, an added strain of 1.02, 1.04, and 2.94 kcal/mol on the acetyl group, central pyranose ring, and glycerol group, respectively, was seen when including crystal waters. This conformational strain is necessary to establish favorable contacts with the protein. When simulations of Relenza were performed without crystal waters, the nonbonded van der Waals and electrostatic interaction energies are not as favorable (data not shown). The better binding Tamiflu rectifies this problem by not having a large conformational dependence on crystal water molecules, thus preventing a large unfavorable internal energy change upon binding.

Tamiflu, unlike the other ligands, samples the same binding position regardless of crystal water molecules after about 400 ps of simulation. The ammonium and ether groups of Tamiflu act as anchors to secure the ligand in the active site reducing its dependence on water (Figure 4). While Relenza's glycerol group shifts significantly, Tamiflu's additional ether group lends stronger packing of Tamiflu into the active site. Our results suggest that Tamiflu's functional groups improve binding by orienting the ligand to take advantage of contacts within the active site and more importantly help to avoid the added internal strain upon binding. It appears that a low-energy conformation of Tamiflu
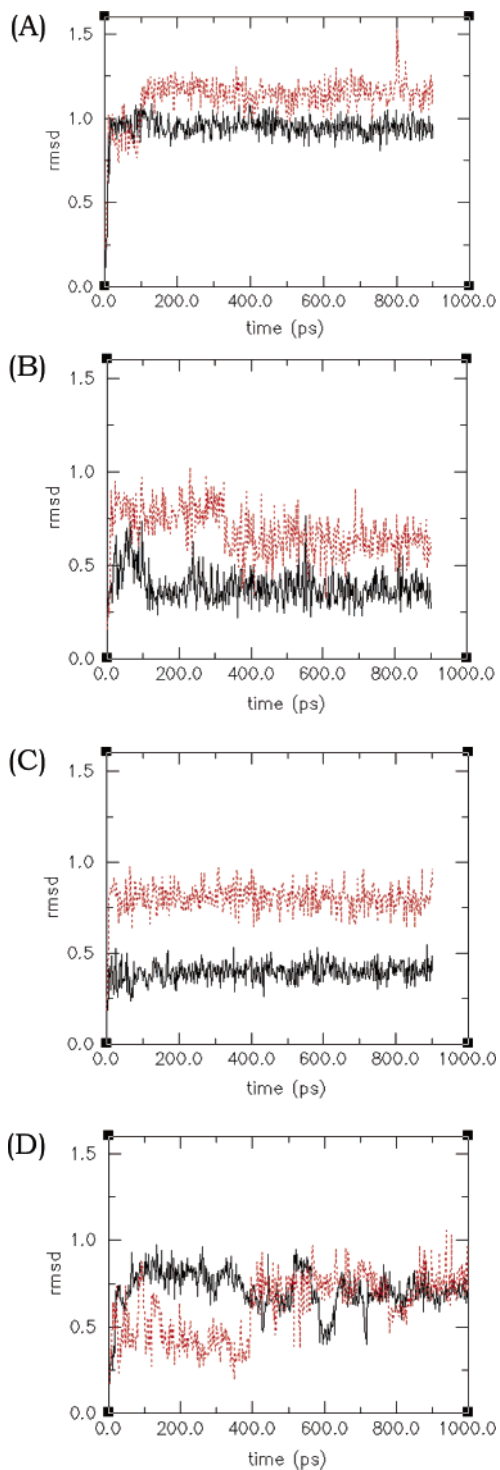
**Figure 2.** All atom RMSD (Å) plots of ligand positions as compared to the initial minimized crystal structures. From top to bottom, (A) sialic acid, (B) DANA, (C) Relenza, (D) Tamiflu. Dashed lines are simulation without crystal waters and solid lines are from simulations that included crystal waters.



**Figure 3.** $C_\alpha$ Overlay of snapshots from Relenza MD trajectory taken with and without crystal waters. White is conformation obtained from simulation with crystal waters, and black is from simulation without crystal waters. Both snapshots are taken from 550 ps into the simulation.



**Figure 4.** $C_\alpha$ Overlay of snapshots from Tamiflu MD trajectory taken with and without crystal waters. White is conformation obtained from simulation with crystal waters, and black is from simulation without crystal waters. Both snapshots are taken from 550 ps into the simulation.

complements the active site better than the highly strained conformation of Relenza.

Recognizing that the free energy of association is a combination of many terms, the loss in electrostatic energy by having charged groups is more than compensated for by gains in other molecular mechanic terms. This is evident by the fact that Relenza and Tamiflu, which both have an additional positively charged group, have neg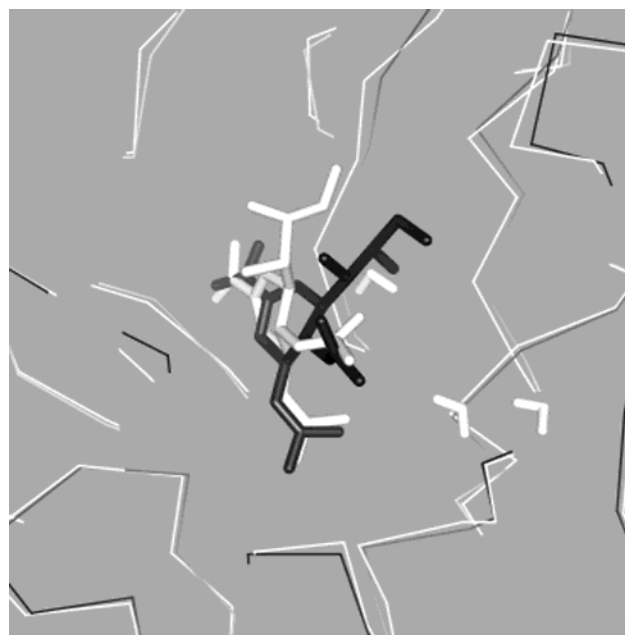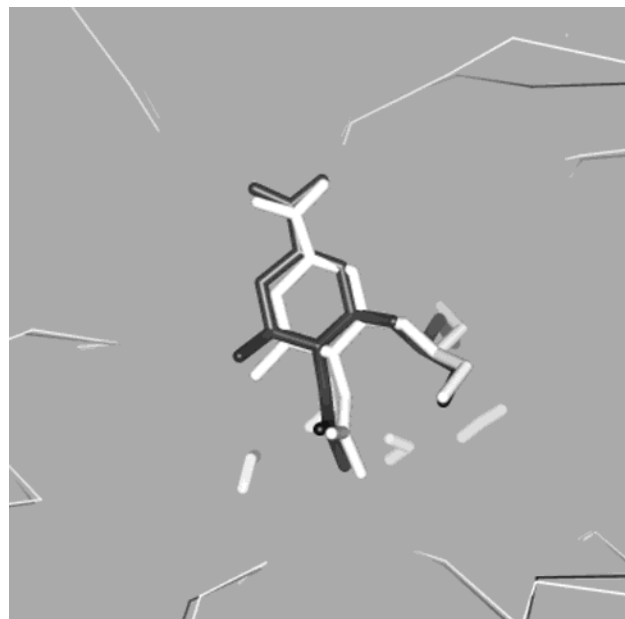ligible or slightly positive electrostatic terms that oppose binding, yet are the two best binders. Work by Chervenak and Toone has shown that the binding of carbohydrates in aqueous solutions results in an entropic gain through the displacement of solvent from the binding pocket.[51] Despite those results, many authors agree that the role of water in protein−ligand binding is complex and necessitates further discussion.[19,44,45,47,52] Our work presented here suggests that water molecules in the neuraminidase active site serve an equally important role of positioning ligand atoms.
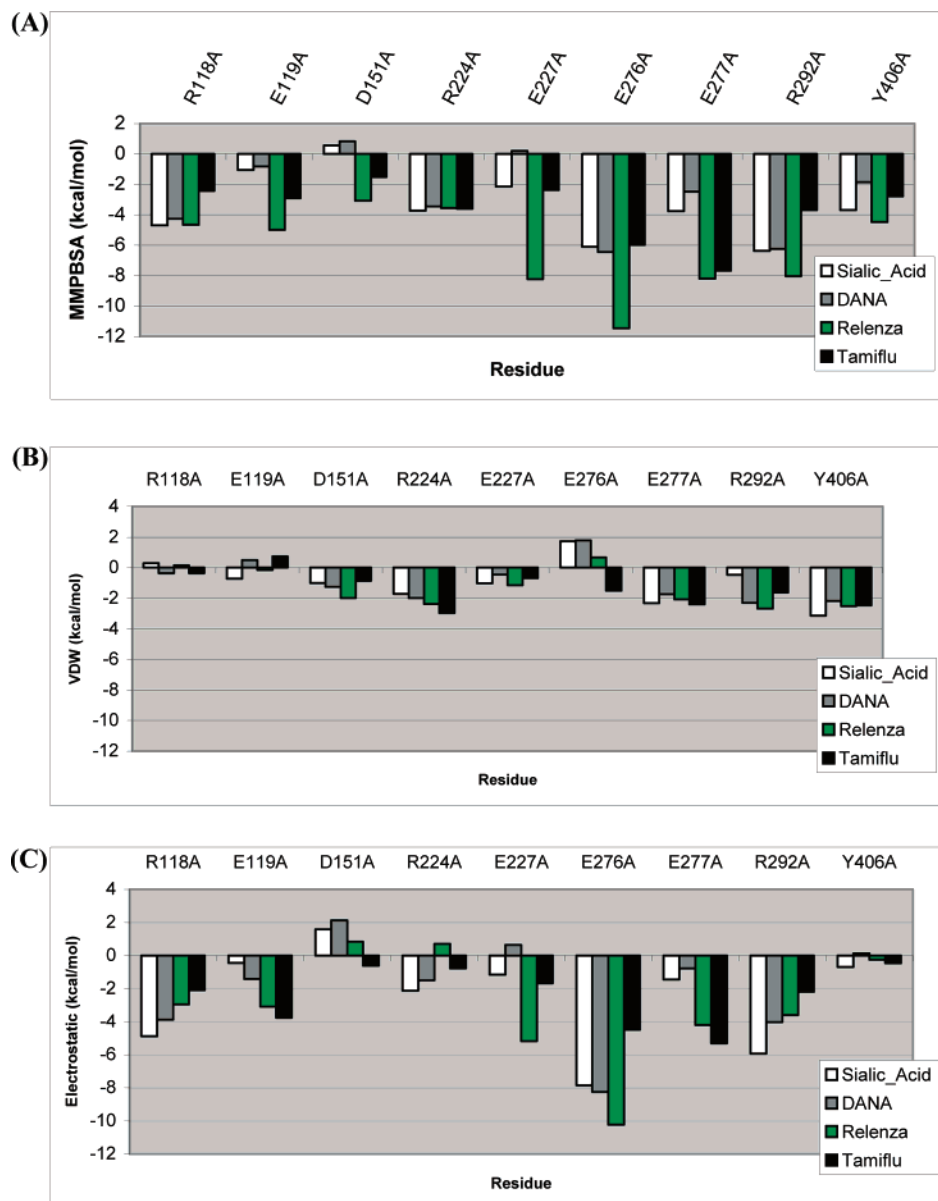
**Figure 5.** Computational alanine-scanning results for neuraminidase with the four ligands. Shown are the relative free energy (kcal/mol) changes obtained from the mutated snapshots averaged over the MD trajectories. Negative free energies ($\Delta\Delta = \Delta_{\text{wildtype}} - \Delta_{\text{mutant}}$) represent an alanine mutation that is unfavorable to binding. (A) $\Delta\Delta G_{\text{binding}}$; (B) $\Delta\Delta E_{\text{VDW}}$; (C) $\Delta\Delta E_{\text{elec,int+solv}}$.

**Alanine-Scanning.** To investigate other factors besides internal intramolecular interactions that may help confer specificity, computational alanine-scanning[53] was employed to probe which residues make a significant intermolecular contribution to the differential in binding. Figure 5 shows our results for alanine mutations made to nine residues in contact with the inhibitors. Negative energetic changes ($\Delta G_{\text{wt}} - \Delta G_{\text{ala}}$) represent an unfavorable substitution. As expected, we see that in general, mutations of active site residues are highly unfavorable with all four inhibitors. However, three residues in the active site are predicted to contribute differentially in binding to these ligands.

Alanine mutations to E119, D151, and E277 show the largest variance in free energy of binding, suggesting that they play a role in substrate selectivity. As seen from Figure 5, while E119 contributes only slightly to binding sialic acid and DANA, Tamiflu and Relenza are able to form much more favorable interactions. Mutagenic studies have supported the notion of E119

**Table 3.** Experimental Fold Resistance (FR) Inhibition Data for an E119A Mutant

| | FR[a] | $\Delta\Delta G_{\text{FR}}$ |
|---|---|---|
| DANA | 7 | −1.17 kcal/mol |
| Relenza | 600 | −3.84 kcal/mol |

[a] Reference 54. FR = E119A/Wildtype.

playing a role in substrate selectivity, where inserting an alanine at this position has shown a 1.17 kcal/mol reduction in binding to DANA while experiencing a 3.84 kcal/mol loss in affinity to Relenza[54] (Table 3). This is in accord with our calculations that show an E119A mutant only alters DANA binding by 0.83 kcal/mol compared to wildtype, while Relenza's affinity is weakened by 5.0 kcal/mol (Figure 5). Our calculations further suggest that this differential is due to the positive electrostatic potential of the extra functional groups on Tamiflu and Relenza acting as an anchor for the negative E119 buried in the active site pocket. Sialic acid and DANA do not have the extra positive charge

off the C4 position. In similar fashion, D151 also helps to confer specificity by establishing stronger interactions with the better binding ligands. The data shows that D151 is not used in binding sialic acid or the structurally similar DANA, but can be exploited with the more potent inhibitors. Ghate found that the $K_i$ for DANA to an D149E (B/Lee/40 numbering) mutant versus wild-type is of the same magnitude, 35 $\mu$M and 53 $\mu$M, respectively.[55] A deeper investigation into the energetic components reveals that the gain in free energy from D151 is from an increased electrostatic energy associated with the positively charged groups on Tamiflu and Relenza interacting with the negative electrostatic potential of the aspartic acid. While there remains a slight electrostatic penalty when binding Relenza, it is still lower than DANA or sialic acid. E277 contributes almost 4 kcal/mol more free energy when binding Tamiflu or Relenza than it does with the other ligands. This glutamate is located on the floor of the binding pocket not in the vicinity of the C4 substituents off the central ring. One possible explanation for the increased interaction, despite being distant from the ammonium or guanidinium groups, could be that the added charge on Tamiflu and Relenza helps to provide their other functional groups better contacts with this residue.

Although this study suggests E119, D151, and E277 help confer specificity, there are other residues that are important for establishing potent interactions with all the ligands. R118, R224, and R292 contribute equally to all four ligands, providing significant free energy to these complexation events. The participation of R118 and R292, both of which surround the common carboxylate moiety on the ligands, is expected. R224 is positioned between the acetyl and glycerol functional groups of the ligands and provides electrostatic and van der Waals free energy to the complexes. Conversely, Y406 provides a marginal free energy gain upon binding for all four ligands. This residue is implicated to be essential for activity of neuraminidase because a phenylalanine mutation at this position shows no activity in fluorescence assays.[55,56] In agreement, results from this study suggest that Y406 may play more of a kinetic or substrate positioning role in catalysis as opposed to a thermodynamic role in binding. This result implies that despite its necessity, targeting Y406 in attempts to increase affinity of potential drug candidates may be futile.

As mentioned earlier, our studies suggested that the tighter binding of Tamiflu and Relenza is explained by stronger van der Waals interactions. From the individual nonpolar contributions listed in Figure 5B, it is difficult to discern which set of residues is responsible for this large van der Waals increase. While E276, which is below the ether moiety, appears to take advantage of the increased nonpolar character of Tamiflu, no set of residues explains the over 6 kcal/mol van der Waals interaction energy difference between strong and weak ligands. E276 experiences a reorganization of its side chain upon binding Tamiflu. Through our alanine-scanning, it appears that this rotation allows neuraminidase more van der Waals interactions with Tamiflu compared to the other three ligands that do not induce a rotation of E276. The fact that this rotation is already present in our starting structures suggests that we have captured some of the energetics associated with E276's rotation, but note that without complete sampling of the free receptor, a true quantitative explanation for the energetic effects of E276 rotation is difficult to draw. As evident in Figure 5, the dispersed nature of van der Waals contacts suggests that targeting a specific hydrophobic residue or pocket to gain selectivity may be difficult. In contrast, while electrostatics, as a whole, fails to segregate ligands, alanine-scanning has shown that individual interactions from residues may be differentiated and as a result can be further targeted to give rise to differences in binding energy (Figure 5C). Alanine-scanning of the neuraminidase active site with the four ligands has uncovered that the main residues contributing to selectivity upon binding are E119, D151, and E277 and suggests that additional mutations at either D151 or E277 would mitigate binding of Tamiflu or Relenza.

## Conclusions

We used molecular dynamic simulations in conjunction with free energy calculations to analyze the binding specificity of the neuraminidase active site to a series of inhibitors and also examined the dynamic nature of ligand binding. MM/PBSA analysis correctly rank-ordered binding affinities and segregated the different energetic components among all four cocrystal complexes permitting a detailed hypothesis on the structural determinants of binding. The calculations suggest that neuraminidase inhibitors take advantage of increased van der Waals interactions to bind the active site better and that overall electrostatic components provide no direct *thermodynamic* advantage, or even oppose complexation, despite a highly polar active site. Alanine-scanning suggests that while electrostatic effects do not contribute to strengthening the affinity nor helping to discriminate strong binders from weak binders, it still plays a vital role in substrate specificity and can be targeted further for drug design. Potency is suggested to be enhanced by the increased charge of the better binding ligands helping to establish and secure scaffold orientations in the active site so that other interactions can be maximized. This point was further supported through simulations with and without crystal water molecules in the active site, that showed that the lack of extra charged or hydrophobic groups caused a larger dependence on water for scaffold positioning in the active site. Recently, others have also noted the importance of a consistent scaffold binding mode for compounds that target neuraminidase.[10] Although electrostatics as a whole provides no net gain to binding, alanine-scanning revealed that an energy differential was present when considering interactions of each ligand with individual charged residues.

This study exemplifies and stresses the importance of considering crystal water molecules in a recognition process. Tamiflu's high affinity is largely explained by its direct binding-site complementarity without the need for mediating water molecules, in contrast to its weaker binding counterparts. Given that many other carbohydrate-binding protein crystal structures have been solved with crystallographic waters present, inclusion of these waters is both feasible and necessary for understanding the interactions in order to develop potent inhibitors.

While this study was able to suggest ways neuraminidase recognizes a series of inhibitors, the power of this technique is its use as an analytical tool and cannot be used in a predictive manner without the implementation of higher sampling techniques. Higher sampling techniques would afford the broader search of the energy landscape and a closer estimate to the energy of each binding partner. The location of water molecules remains an issue in computational biology and hinders predictive studies of neuraminidase recognition.

**Supporting Information Available:** Structures, partial charges, AMBER atom types, and additional force field parameters used for each ligand. This material is available free of charge via the Internet at http://pubs.acs.org.

## References

(1) Sears, P.; Wong, C. H. Carbohydrate mimetics: A new strategy for tackling the problem of carbohydrate-mediated biological recognition. *Angew. Chem., Int. Ed.* **1999**, *38*, 2301−2324.

(2) Paulson, J. C. The Receptors. In *The Receptors*; Conn, P. M., Ed.; Academic Press: Orlando, FL, 1984; pp 131−219.

(3) Huang, R. T.; Rott, R.; Klenk, H. D. Influenza viruses cause hemolysis and fusion of cells. *Virology* **1981**, *110*, 243−247.

(4) Colman, P. M. The Influenza viruses. In *The Viruses*; Krug, R. M., Ed.; Plenum Press: New York, 1989; pp 175−218.

(5) Bodian, D. L.; Yamasaki, R. B.; Buswell, R. L.; Stearns, J. F.; White, J. M. et al. Inhibition of the fusion-inducing conformational change of influenza hemagglutinin by benzoquinones and hydroquinones. *Biochemistry* **1993**, *32*, 2967−2978.

(6) Bamford, M. J. Neuraminidase inhibitors as potential antiinfluenza drugs. *J. Enzyme Inhib.* **1995**, *10*, 1−16.

(7) Weinhold, E. G. Design and Evaluation of a Tightly Binding Fluorescent Ligand for Influenza A Hemagglutinin. *J. Am. Chem. Soc.* **1992**, *114*, 9270−9275.

(8) Babu, Y. S.; Chand, P.; Bantia, S.; Kotian, P.; Dehghani, A. et al. BCX-1812 (RWJ-270201): Discovery of a novel, highly potent, orally active, and selective influenza neuraminidase inhibitor through structure-based drug design. *J. Med. Chem.* **2000**, *43*, 3482−3486.

(9) Wang, G. T.; Chen, Y. W.; Wang, S.; Gentles, R.; Sowin, T. et al. Design, synthesis, and structural analysis of influenza neuraminidase inhibitors containing pyrrolidine cores. *J. Med. Chem.* **2001**, *44*, 1192−1201.

(10) Stoll, V.; Stewart, K. D.; Maring, C. J.; Muchmore, S.; Giranda, V. et al. Influenza neuraminidase inhibitors: structure-based design of a novel inhibitor series. *Biochemistry* **2003**, *42*, 718−727.

(11) Gubareva, L. V.; Kaiser, L.; Hayden, F. G. Influenza virus neuraminidase inhibitors. *Lancet* **2000**, *355*, 827−835.

(12) Smith, P. W.; Sollis, S. L.; Howes, P. D.; Cherry, P. C.; Cobley, K. N. et al. Novel inhibitors of influenza sialidases related to GG167 − Structure−activity, crystallographic and molecular dynamic studies with 4H-pyran-2-carboxylic acid 6-carboxamides. *Bioorg. Med.Chem. Lett.* **1996**, *6*, 2931−2936.

(13) White, C. L.; Janakiraman, M. N.; Laver, W. G.; Philippon, C.; Vasella, A. et al. A sialic acid-derived phosphonate analogue inhibits different strains of influenza virus neuraminidase with different efficiencies. *J. Mol. Biol.* **1995**, *245*, 623−634.

(14) Vonitzstein, M.; Wu, W.; Kok, G. B.; Pegg, M. S.; Dyason, J. C. et al. Rational Design of Potent Sialidase-Based Inhibitors of Influenza Virus Replication. *Nature* **1993**, *363*, 418−423.

(15) Jedrzejas, M. J.; Singh, S.; Brouillette, W. J.; Air, G. M.; Luo, M. A Strategy for Theoretical Binding Constant, K−I, Calculations for Neuraminidase Aromatic Inhibitors Designed on the Basis of the Active Site Structure of Influenza Virus Neuraminidase. *Proteins* **1995**, *23*, 264−277.

(16) Potier, M.; Mameli, L.; Belisle, M.; Dallaire, L.; Melancon, S. B. Fluorometric assay of neuraminidase with a sodium (4-methylumbelliferyl- alpha-D-N-acetylneuraminate) substrate. *Anal. Biochem* **1979**, *94*, 287−296.

(17) Finley, J. B.; Atigadda, V. R.; Duarte, F.; Zhao, J. J.; Brouillette, W. J. et al. Novel aromatic inhibitors of influenza virus neuraminidase make selective interactions with conserved residues and water molecules in the active site. *J. Mol. Biol.* **1999**, *293*, 1107−1119.

(18) Chand, P.; Kotian, P. L.; Dehghani, A.; El-Kattan, Y.; Lin, T. H. et al. Systematic structure-based design and stereoselective synthesis of novel multisubstituted cyclopentane derivatives with potent antiinfluenza activity. *J. Med. Chem.* **2001**, *44*, 4379−4392.

(19) Wang, T.; Wade, R. C. Comparative binding energy (COMBINE) analysis of influenza neuraminidase-inhibitor complexes. *J. Med. Chem.* **2001**, *44*, 961−971.

(20) Vonitzstein, M.; Dyason, J. C.; Oliver, S. W.; White, H. F.; Wu, W. Y. et al. A Study of the Active Site of Influenza Virus Sialidase − an Approach to the Rational Design of Novel Anti-Influenza Drugs. *J. Med. Chem.* **1996**, *39*, 388−391.

(21) Jayaram, B.; Sprous, D.; Young, M. A.; Beveridge, D. L. Free Energy Analysis of the Conformational Preferences of a and B Forms of DNA in Solution. *J. Am. Chem. Soc.* **1998**, *120*, 10629−10633.

(22) Vorobjev, Y. N.; Almagro, J. C.; Hermans, J. Discrimination Between Native and Intentionally Misfolded Conformations of Proteins − ES/IS, A New Method for Calculating Conformational Free Energy That Uses Both Dynamics Simulations With an Explicit Solvent and an Implicit Solvent Continuum Model [Review]. *Proteins* **1998**, *32*, 399−413.

(23) Kollman, P. A.; Massova, I.; Reyes, C.; Kuhn, B.; Huo, S. H. et al. Calculating structures and free energies of complex molecules: Combining molecular mechanics and continuum models. *Acc. Chem. Res.* **2000**, *33*, 889−897.

(24) Chong, L. T.; Duan, Y.; Wang, L.; Massova, I.; Kollman, P. A. Molecular dynamics and free-energy calculations applied to affinity maturation in antibody 48G7. *Proc. Natl. Acad. Sci. U. S. A.* **1999**, *96*, 14330−14335.

(25) Huo, S. H.; Wang, J. M.; Cieplak, P.; Kollman, P. A.; Kuntz, I. D. Molecular dynamics and free energy analyses of cathepsin D-inhibitor interactions: Insight into structure-based ligand design. *J. Med. Chem.* **2002**, *45*, 1412−1419.

(26) Gouda, H.; Kuntz, I. D.; Case, D. A.; Kollman, P. A. Free energy calculations for theophylline binding to an RNA aptamer: MM-PBSA and comparison of thermodynamic integration methods. *Biopolymers* **2003**, *68*, 16−34.

(27) Pearlman, D. A.; Case, D. A.; Caldwell, J. W.; Ross, W. S.; Cheatham, T. E. et al. Amber, a Package of Computer Programs for Applying Molecular Mechanics, Normal-Mode Analysis, Molecular Dynamics and Free Energy Calculations to Simulate the Structural and Energetic Properties of Molecules. *Comput. Phys. Commun.* **1995**, *91*, 1−41.

(28) Varghese, J. N.; Colman, P. M.; van Donkelaar, A.; Blick, T. J.; Sahasrabudhe, A. et al. Structural evidence for a second sialic acid binding site in avian influenza virus neuraminidases. *Proc. Natl. Acad. Sci. U. S. A.* **1997**, *94*, 11808−11812.

(29) Smith, B. J.; Colman, P. M.; Von Itzstein, M.; Danylec, B.; Varghese, J. N. Analysis of inhibitor binding in influenza virus neuraminidase. *Protein Sci.* **2001**, *10*, 689−696.

(30) Varghese, J. N.; Epa, V. C.; Colman, P. M. Three-dimensional structure of the complex of 4-guanidino-Neu5Ac2en and influenza virus neuraminidase. *Protein Sci.* **1995**, *4*, 1081−1087.

(31) Varghese, J. N.; Smith, P. W.; Sollis, S. L.; Blick, T. J.; Sahasrabudhe, A. et al. Drug design against a shifting target: a structural basis for resistance to inhibitors in a variant of influenza virus neuraminidase. *Structure* **1998**, *6*, 735−746.

(32) Jorgensen, W. L.; Chandrasekhar, J.; Madura, J. D.; Impey, R. W.; Klein, M. L. Comparison of simple potential functions for simulating liquid water. *J. Chem. Phys.* **1983**, *79*, 926−935.

(33) Bayly, C. I.; Cieplak, P.; Cornell, W. D.; Kollman, P. A. A Well-Behaved Electrostatic Potential Based Method Using Charge Restraints for Deriving Atomic Charges − the Resp Model. *J. Phys. Chem.* **1993**, *97*, 10269−10280.

(34) Frisch, M. J.; Trucks, G. W.; Schlegel, H. B.; Scuseria, G. E.; Robb, M. A.; Cheeseman, J. R.; Zakrzewski, V. G.; Montgomery, J. A., Jr.; Stratmann, R. E.; Burant, J. C.; Dapprich, S.; Millam, J. M.; Daniels, A. D.; Kudin, K. N.; Strain, M. C.; Farkas, O.; Tomasi, J.; Barone, V.; Cossi, M.; Cammi, R.; Mennucci, B.; Pomelli, C.; Adamo, C.; Clifford, S.; Ochterski, J.; Petersson, G. A.; Ayala, P. Y.; Cui, Q.; Morokuma, K.; Malick, D. K.; Rabuck, A. D.; Raghavachari, K.; Foresman, J. B.; Cioslowski, J.; Ortiz, J. V.; Stefanov, B. B.; Liu, G.; Liashenko, A.; Piskorz, P.; Komaromi, I.; Gomperts, R.; Martin, R. L.; Fox, D. J.; Keith, T.; Al-Laham, M. A.; Peng, C. Y.; Nanayakkara, A.; Gonzalez, C.; Challacombe, M.; Gill, P. M. W.; Johnson, B. G.; Chen, W.; Wong, M. W.; Andres, J. L.; Head-Gordon, M.; Replogle, E. S.; Pople, J. A. *Gaussian 98*, revision A7; Gaussian, Inc.: Pittsburgh, PA, 1998.

(35) Cornell, W. D.; Cieplak, P.; Bayly, C. I.; Gould, I. R.; Merz, K. M. et al. A Second Generation Force Field for the Simulation of Proteins, Nucleic Acids, and Organic Molecules. *J. Am. Chem. Soc.* **1995**, *117*, 5179−5197.

(36) Ryckaert, J. P.; Ciccotti, G.; Berendsen, H. J. C. Numerical integration of the Cartesian equations of motion of a system with constraints: molecular dynamics of *n*-alkanes. *J. Comput. Phys.* **1977**, *23*, 327−341.

(37) Levy, R. M.; Karplus, M.; Kushick, J.; Perahia, D. Evaluation of the Configurational Entropy for Proteins: Application to Molecular Dynamics Simulations of an α-Helix. *Macromolecules* **1984**, *17*, 1370−1374.

(38) Hayward, S.; Kitao, A.; Go, N. Harmonicity and anharmonicity in protein dynamics: a normal-mode analysis and principal component analysis. *Proteins* **1995**, *23*, 177−186.

(39) Case, D. A. Normal-Mode Analysis of Protein Dynamics. *Curr. Opin. Struct. Biol.* **1994**, *4*, 285−290.

(40) Sharp, K. A.; Honig, B. Electrostatic Interactions in Macromolecules − Theory and Applications. *Annu. Rev. Biophys. Biophys. Chem.* **1990**, *19*, 301−332.

(41) Lee, M. R.; Tsai, J.; Baker, D.; Kollman, P. A. Molecular Dynamics in the Endgame of Protein Structure Prediction. *J. Mol. Biol.* **2001**, *313*, 417−430.

(42) Sanner, M. F.; Olson, A. J.; Spehner, J. C. Reduced Surface − an Efficient Way to Compute Molecular Surfaces. *Biopolymers* **1996**, *38*, 305−320.

(43) Sitkoff, D.; Sharp, K. A.; Honig, B. Accurate Calculation of Hydration Free Energies Using Macroscopic Solvent Models. *J. Phys. Chem.* **1994**, *98*, 1978−1988.

(44) Wall, I. D.; Leach, A. R.; Salt, D. W.; Ford, M. G.; Essex, J. W. Binding constants of neuraminidase inhibitors: An investigation of the linear interaction energy method. *J. Med. Chem.* **1999**, *42*, 5142−5152.

(45) Taylor, N. R.; Vonitzstein, M. A Structural and Energetics Analysis of the Binding of a Series of N−Acetylneuraminic-Acid-Based Inhibitors to Influenza Virus Sialidase. *Journal of Computer-Aided Molecular Design* **1996**, *10*, 233−246.

(46) Smith, B. J. A Conformational Study of 2-Oxanol − Insight into the Role of Ring Distortion on Enzyme-Catalyzed Glycosidic Bond Cleavage. *J. Am. Chem. Soc.* **1997**, *119*, 2699−2706.

(47) Clarke, C.; Woods, R. J.; Gluska, J.; Cooper, A.; Nutley, M. A. et al. Involvement of water in carbohydrate-protein binding. *J. Am. Chem. Soc.* **2001**, *123*, 12238−12247.

(48) Swaminathan, C. P.; Surolia, N.; Surolia, A. Role of water in the specific binding of mannose and mannooligosaccharides to concanavalin A. *J. Am. Chem. Soc.* **1998**, *120*, 5153−5159.

(49) Ladbury, J. E. Just add water! The effect of water on the specificity of protein−ligand binding sites and its potential application to drug design. *Chemistry & Biology* **1996**, *3*, 973−980.

(50) Toone, E. J. Structure and Energetics of Protein Carbohydrate Complexes. In *Current Opinion in Structural Biology*, 1994; pp 719−728.

(51) Chervenak, M. C.; Toone, E. J. A Direct Measure of the Contribution of Solvent Reorganization to the Enthalpy of Ligand Binding. *J. Am. Chem. Soc.* **1994**, *116*, 10533−10539.

(52) Smith, B. J.; McKimm-Breshkin, J. L.; McDonald, M.; Fernley, R. T.; Varghese, J. N. et al. Structural studies of the resistance of influenza virus neuramindase to inhibitors. *J. Med. Chem.* **2002**, *45*, 2207−2212.

(53) Massova, I.; Kollman, P. A. Computational alanine scanning to probe protein−protein interactions: A novel approach to evaluate binding free energies. *J. Am. Chem. Soc.* **1999**, *121*, 8133−8143.

(54) Gubareva, L. V.; Robinson, M. J.; Bethell, R. C.; Webster, R. G. Catalytic and framework mutations in the neuraminidase active site of influenza viruses that are resistant to 4-guanidino-Neu5Ac2en. *J. Virol.* **1997**, *71*, 3385−3390.

(55) Ghate, A. A.; Air, G. M. Site-directed mutagenesis of catalytic residues of influenza virus neuraminidase as an aid to drug design. *Eur. J. Biochem.* **1998**, *258*, 320−331.

(56) Janakiraman, M. N.; White, C. L.; Laver, W. G.; Air, G. M.; Luo, M. Structure of Influenza Virus Neuraminidase B/Lee/40 Complexed with Sialic Acid and a Dehydro Analogue at 1.8-Angstrom Resolution − Implications for the Catalytic Mechanism. *Biochemistry* **1994**, *33*, 8172−8179.